Doerr, Martin and Apostolis Sarris (eds) 2003. The Digital Heritage of Archaeology. CAA2002. Computer Applications and Quantitative Methods in Archaeology. Proceedings of the 30th CAA Conference, Heraklion, Crete, April 2002.

High Resolution Geophysical Imaging of Buried Relics in Itanos Archaeological Site

Antonios Vafidis[1], George Poulioudis[1], George Kritikakis[1] and Apostolos Sarris[2]

[1] Applied Geophysics Lab, Technical University Of Crete, Chania 73100, Greece
vafidis@mred.tuc.gr, gpouliou@geoph.tuc.gr, gkritik@geoph.tuc.gr
[2]Laboratory of Geophysical-Satellite Remote Sensing and Arcaeo-environment,
Institute of Mediterranean Studies-Foundation for Research and Technology, Hellas
(F.O.R.T.H.), Melissinou and Nikiforou Foka 130, PO. Box 119, Rethymnon 74100, Crete, Greece.
asaris@ret.forthnet.gr

Abstract. Non-invasive high-resolution geophysical techniques, such as ground penetrating radar (GPR), electrical tomography and seismics, have been applied in archaeological investigations during a geophysical survey, which took place in the archaeological site of Itanos in Greece. The main objective of survey was to delineate the remains of buried relics in selected areas by combining these high-resolution geophysical methods. Three sets of GPR antennas were employed to achieve optimal system performance. GPR time slices, presented in a series of maps and electrical tomography resistivity sections revealed features at different depths related to soil resistance and magnetic gradient anomalies, attributed to buried relics of building walls. In particular, in the ancient harbor compatible results were obtained from seismic refraction, surface waves, GPR, electrical tomography and other geophysical methods, indicating that the depth to the bedrock is varying from 2 to 10 m.
Keywords. GPR, surface waves, electrical tomography, S-waves, archaeology

1 Introduction

A geophysical survey was carried out in the archaeological site of Itanos (Crete) to explore the usefulness of combining geophysical mapping and imaging techniques in delineating shallow targets of archaeological interest.

Itanos, an ancient coastal site in Eastern Crete, is located 10 km north of Palaikastro, Lasithi prefecture, close to the unique in Europe Vai Palm Forest. There are two acropolis in Itanos. Most of the relics of the buildings of the ancient city are located in the region between the acropolis. Itanos is marked mainly from three periods: Geometric, Roman and Early Byzantine, while the periods of original occupation and abandonment are not known. An archaeological collaborative campaign between the French School of Archaeology in Athens and the Institute of Mediterranean Studies FORTH was initiated in the area in 1993. Within the context of archaeological investigations, a geophysical prospecting expedition was also carried out.

Apart from the conventional geophysical methods namely the soil resistance, the magnetic gradient and the electromagnetic mapping, the following methods were employed on selected grids:

(a) Shallow seismics employing the seismic refraction and surface wave methods.
(b) Ground Penetrating Radar with 110 MHz, 225 MHz and 450 MHz antennas of a pulse EKKO 1000 GPR system.
(c) 2D electrical tomography using the Wenner, dipole-dipole or the pole-pole arrays.

2 Seismic Survey in Itanos Site

The archaeological site of Itanos is located at the eastern part of the island of Crete (S. Greece) (Fig. 1). A seismic survey, conducted by the Laboratory of Applied Geophysics in September 2002, included 3 seismic lines L_1, L_3 and L_4 (Fig. 1). Apart from this survey, several others have been conducted at the same area in order to map the bedrock relief and to examine the existence of the old harbor. The seismic survey described in this work was applied to compare conventional (refraction) and non-conventional (surface waves) seismic methods for the determination of the variation of the S-wave velocity distribution with depth. The S-waves are very useful in delineating the water-saturated layers.

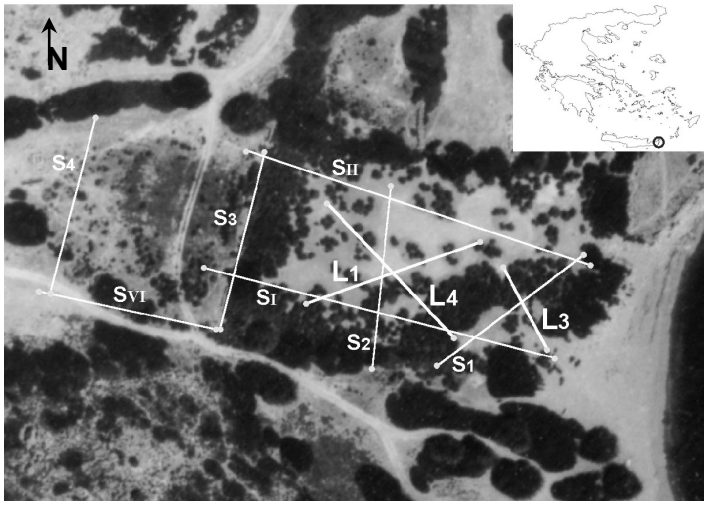

Fig. 1. *Seismic lines from surveys, conducted at the archaeological site of Itanos in order to map the bedrock relief and to examine the existence of the old harbor.*

The seismic survey employed the refraction method (both for P and S-waves) as well as the surface wave inversion method. In particular, line L_1 was scanned with P and S-wave refraction methods, whereas line L_4, with only P-wave refraction and surface waves method.

2.1 P-wave refraction

From previous surveys, conducted at the same area, it was found that the subsurface consists of three layers (Vafidis et al., 2002):

1. A thin layer of loose, dry sand with thickness of 1.5–2 m. Its P-wave velocity has a value of about 400 m/s.
2. An intermediate layer of saturated clayey soil. The thickness of this layer is variable. The mean thickness is 10 m and the P-wave velocity about 1700 m/s.
3. The eroded bedrock of the area consists of phyllites-quarzites with P-wave velocity approximately 2500 m/s.

The field parameters are summarized on Table 1. The data were processed using the ray-tracing technique (Haeni et al., 1987). The results for the three seismic lines (L_1, L_3 and L_4) are cited on Table 2, whereas the cross-section of L_1 and L_4 depth sections, in Figure 2. These results are compatible to those deduced from previous surveys.

Active geophones	24
Frequency	14 Hz (Land Mark)
Geophone spacing	2 m (1 m for L_3)
Middle shot offset	1 m (0.5 m for L_3)
Near shot offset	2 m (1 m for L_3)
Far shot offset	Variable
Sampling rate	0.1 ms
Record length	204 ms
Filter	50 Hz (notch filter)
Seismic source	Sledgehammer 5 kg
Seismograph	ES-2401 Geometrics

Table 1. *Record parameters for the P-wave refraction survey.*

Seismic line	Layer	Description	Mean Vp (m/sec)	Mean thickness (m)
L_1	**1**	Dry sand	382	1.19
	2	Saturated clayey soil	1728	7.27
	3	Bedrock: Eroded phyllites	2785	-
L_3	**1**	Dry sand	416	1.59
	2	Saturated clayey soil	1705	5.19
	3	Bedrock: Eroded phyllites	2197	-
L_4	**1**	Dry sand	263	0.85
	2	Saturated clayey soil	1592	7.59
	3	Bedrock: Eroded phyllites	3018	-

Table 2. *Results of the P-wave refraction data, processed using the ray-tracing technique for the three seismic lines (L_1, L_3, L_4).*

2.2 S-wave refraction

S-wave refraction survey was carried out only along seismic line L_1. Two 23 m long spreads with geophone spacing of 1 m were utilized to cover line L_1. Apart from the geometry, almost all parameters were kept the same, as in the experiment of P-wave refraction. The seismic source consisted of a base plate and a large mass placed on top of the plate to provide coupling with the ground. The seismograms obtained by striking the plate on opposite sides, are subtracted in order to remove the P-waves. More than a pair of shots were required to increase the signal to noise ratio.

The results of the S-wave refraction survey, deduced from the records processed with the ray-tracing technique, are presented on Table 3, while Figure 3 displays the depth section. There is a slight difference between the depth sections deduced from the P and S-wave refraction surveys for line L_1. Namely, the second interface is not well imaged by the S-waves due to small number of seismic rays from the second interface (top of eroded bedrock).

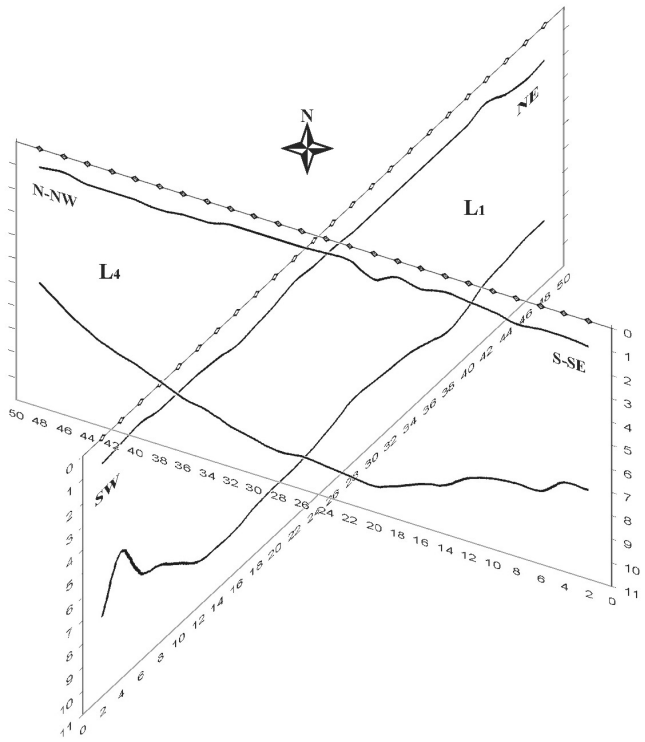

Fig. 2. *Cross-section of L_1 and L_4 depth sections, deduced from the P-wave refraction survey.*

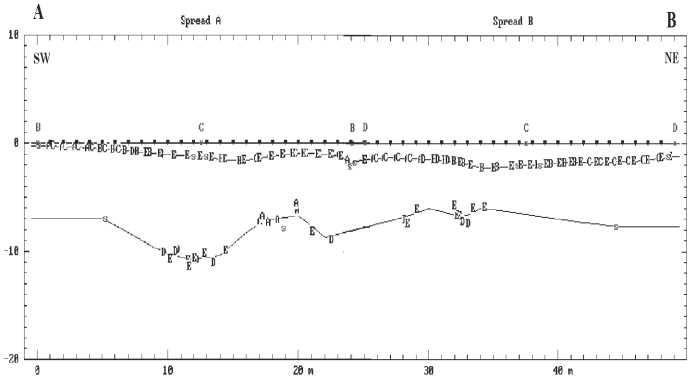

Fig. 3. *Depth section for the seismic line L_1 deduced from the S-wave refraction survey.*

Seismic line	Layer	Description	Mean Vs (m/sec)	Mean thickness (m)
L_1	**1**	Dry sand	150	1.34
	2	Saturated clayey soil	392	7.69
	3	Bedrock: Eroded phyllites	650	-

Table 3. *Results of the S-wave refraction survey, processed using the ray-tracing technique for the seismic line L1.*

2.3 Surface Wave Survey

Surface Wave Analysis. Recently, in seismic surveys, apart from body waves, surface waves are also studied. The wavefield transformation of Rayleigh surface waves is used for the determination of dispersion curves, which represent the variation of phase velocity of surface waves with frequency. The dispersion curves of different modes, i.e. waveforms of specific velocity that get maximum seismic energy at different frequencies, are commonly named as fundamental and higher (higher velocities at low frequencies) modes.

The phase velocity of Rayleigh surface waves, traveled through horizontally layered medium, is a function of the frequency and four other parameters (Schwab and Knopoff, 1972):

- P-wave velocity
- S-wave velocity
- Density
- Thickness

S-wave velocity (Vs) influences the dispersion curves much more than the rest parameters for frequencies greater than 5 Hz. (Xia, et al., 1999). This is why Vs is better resolved from surface waves analysis than the rest parameters.

Thus, through wavefield transformation and determination of a theoretical dispersion curve, it is possible to estimate the S-wave velocity distribution.

This procedure can be briefly described in three steps:

1. Acquisition (> 5 Hz) of broadband ground roll.
2. Rayleigh wave dispersion curve analysis from ground roll.
3. Inversion of the dispersion curve to obtain near-surface S-wave velocity profiles.

The surface waves survey was conducted along two seismic lines (L_1 and L_4). Actually, this survey was carried out keeping the same field parameters as in the P-wave refraction experiment (Table 1), except the sampling rate and the record length, which were set to 0.5 ms and 1024 ms respectively.

Surface Wave Processing. The extraction of dispersion curves from the raw data was achieved using the seismic software ProMax 2D of Advanced Geophysical Corporation. The processing flow, used for the determination of dispersion curves, after the transformation of data from SEG2 to SEGY format, is briefly described in the following steps:

Disk data input
Trace Header Math (offset correction)
Resample-Desample (change of sampling rate)
Bandpass Filter[1] (to reduce undesirable seismic energy)
Tau – P Transform (slant stacking)
Interactive Spectral Analysis (to perform 1D FFT to Tau)

It was very difficult to identify the dispersion curves after processing, due to low resolution which is related to unsuitable planning of the surface waves survey, namely, not proper geophone spacing and use of notch filter at 50 Hz. From the slowness – frequency diagram, only the fundamental mode dispersion curve can be somehow extracted (Fig.4). Notch filter effects degraded the signal at a zone around 50 Hz and proved fatal for the surface waves analysis. Moreover, the concentration of high seismic energy at the region of 18 – 25 Hz and 4000 – 6000 ms/km prevents from providing a better fundamental dispersion curve. Thus, application of band pass filter (30-35-90-100) improved the dispersion curve extraction.

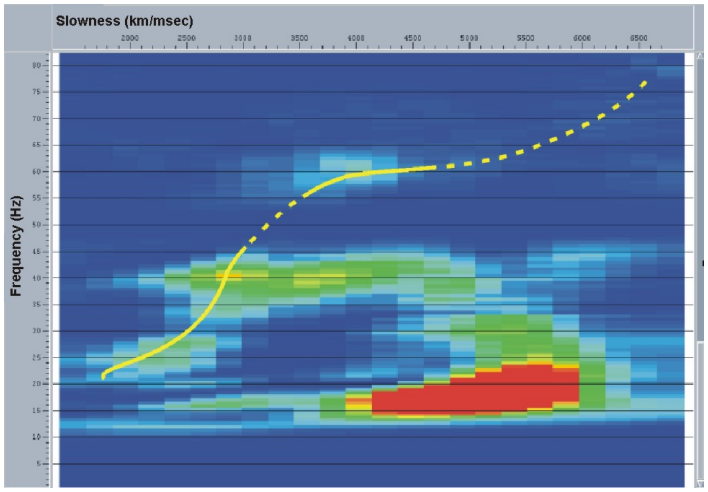

Fig. 4. *Fundamental mode dispersion curve on slowness – frequency diagram. Notch filter effects degraded the signal at a zone around 50 Hz. The dashed parts of dispersion curve correspond to curve extrapolation.*

Inversion of Surface Wave Data. During the inversion procedure, two initial models were introduced. The thickness and P-wave velocity were taken from the P-wave refraction survey, and soil density from bibliography (Telford, et al., 1976). The S-wave velocities for model 1 were set far from the expected values, in order to test the algorithm, whereas the S-wave velocities for model 2 were those deduced from the S-wave refraction survey. The inversion results are presented on Table 4. The results for model 1 led to a better fit between observed and calculated dispersion curves (Fig. 5). However, only the S-wave velocity of the first layer changes for different initial models.

[1] Partially activated

Model	Layer Description	1 Dry sand	2 Saturated clayey soil	3 Eroded phyllites
1	**Thickness (m)**	0.84	7.36	-
	Density ρ	1.6	2.3	2.65
	Vp (m/sec)	263	1594	3008
	Vs (m/sec) (initial)	100	500	900
	Vs (m/sec) (final)	**121.44**	**400.955**	**715.97**
2	**Thickness (m)**	0.84	7.36	-
	Density ρ	1.6	2.3	2.65
	Vp (m/sec)	263	1594	3008
	Vs (m/sec) (initial)	154	392	650
	Vs (m/sec) (final)	**219.78**	**403.040**	**715.39**

Table 4. *Surface wave inversion results for initial models 1 and 2.*

This is possibly caused by the lack in picking the high frequency-low velocity part of observed dispersion curve, which corresponds to the near-surface soil layer. The lack of resolution of the dispersion curve part, which corresponds to the first layer, is mainly caused by the large geophone spacing (2 m) compared to the small thickness of the near-surface layer (0.84 m). Thus, wavelengths of 1 m, which contain information about the first layer, cannot be resolved. However, in general, the S-wave velocities, calculated from the inversion of surface wave data agree with those, calculated from the S-wave refraction survey (especially the velocity of second layer).

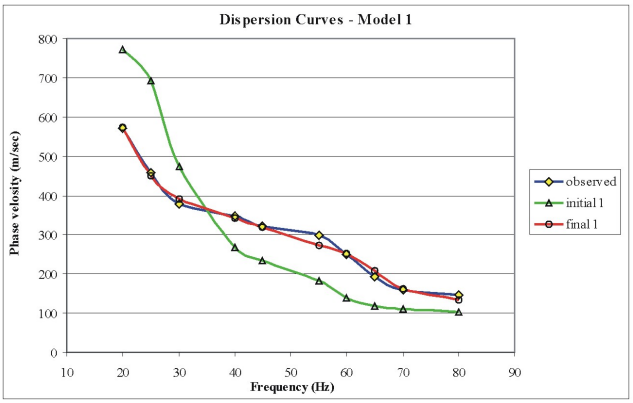

Fig. 5. *Inversion results. Dispersion curves for model 1.*

3 Ground Penetrating Radar and Electrical Tomography

The GPR method is employed to investigate structures at very shallow depths using radio waves within a frequency band from about 1 to 1000 MHz. This technique generates a continuous profile of the subsurface and is applied in finding water table depth, mapping soil stratigraphy and subsurface bedrock topography, locating buried pipes and cables, finding metal and non-metal objects, and detecting caves, tunnels, shafts, fractures and discontinuities.

Ground penetrating radar systems transmit a short pulse of radio frequency (electromagnetic) energy from an antenna (transmitter) into the ground. When electromagnetic energy encounters a subsurface electrical discontinuity part of the energy is reflected and part is propagated across the interface. The total travel time of the transmitted signal to the reflecting interface and back on the surface to the receiver, as well as the amplitude of the returning signal are measured. The amount of energy reflected at a discontinuity depends upon the contrast between the relative dielectric constant (ε_1) and the electrical conductivity (σ) of the target and the soil. Single fold reflection profiling mode is the most common mode to map underlying stratigraphy. In this case receiver and transmitter antennas move along the survey line with a specific orientation and constant separation.

Electrical tomography can be used to map areas with complex subsurface geology where conventional resistivity sounding or profiling surveys are inadequate (Loke and Barker, 1995). It employs a number of electrodes laid out with consecutive address numbering. A computer-controlled system is used to select automatically the active electrodes used for each measurement. Electrical tomography in two dimensions can be performed with several electrode configurations. The data from these surveys are arranged and contoured in the form of a pseudosection, which gives an approximate picture of the subsurface resistivity. The next step is the inversion of the measured apparent resistivity data into true resistivity, which is necessary for accurate depth determination and interpretation.

The inversion program is based on the smoothness constrained least- squares method. The optimization method basically tries to reduce the difference between the calculated and measured apparent resistivity values by adjusting the resistivity of the model blocks. A measure of the difference is given by the root mean squared (RMS) error.

4 Results

Line S_4 (Fig. 1) was scanned with the GPR, electrical tomography and seismic refraction methods. The radar section employing the 110 MHz antennas showed a reflector at 40 – 60ns corresponding probably to the top of the eroded phyllites (Fig. 6a). This reflector is consistent with the interface at 1.5 to 2 m depth on the seismic section (Fig. 6b). On the seismic section, there is also a deeper interface from the top of the phyllites that shows a pit. This pit is also imaged by the electrical tomography method and corresponds to the 30 Ohm·m contour (depth 5 – 8 m, horizontal distance 10 – 34 m) on the resistivity section of Figure 6c. It is worth noting the very shallow (less than 1.5 m) high resistivity anomalies at horizontal distances 12 – 16 m, attributed, according to soil resistance mapping, to anthropogenic buried relics.

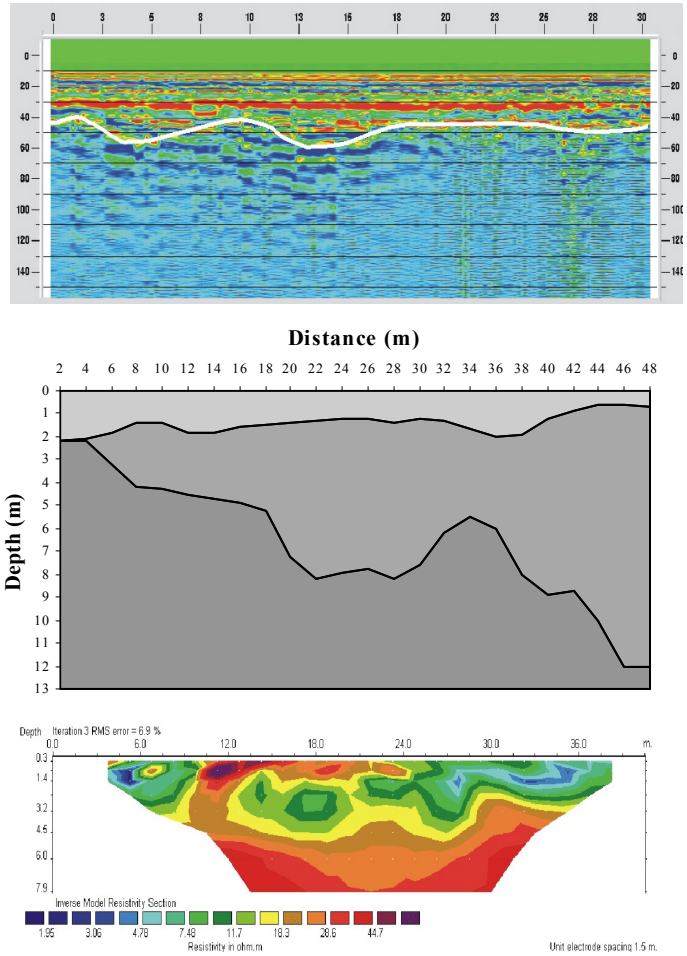

Fig. 6. *The radar section for line S_4 showed a reflector at 40 – 60 ns (vertical axis) corresponding probably to the top of the eroded phyllites (a). This reflector is consistent with the interface at 1.5 to 2 m depth on the seismic section (b). The pit, shown on the seismic section (distance 10 – 34 m), is also imaged by the electrical tomography method on the resistivity section (c).*

The results from P-wave refraction studies indicate that the top of bedrock, consisting of eroded phyllites, reaches a maximum depth of 10 m below the lines L_1 and L_4 (Fig. 2), while it exhibits depths less than 2 m to the west (line S_4, Fig. 6b). This indicates that the potential area of Itanos port, covered by recent deposits, extents approximately 100 m to the west of the present seashore.

The geophysical prospection employed the GPR method in a 30 x 30 m grid A (Fig. 7). Grid A was scanned with 225 MHz and 450 MHz antennas, along closely spaced (0.5 m) parallel survey lines with direction West to East. The station spacing was set to 0.05 m for the 450 MHz antennas and to 0.1 m for the 225 MHz antennas. Selected time slices were extracted from the 225 MHz radar data. Slices exhibit horizontal variation of the reflected wave amplitudes at specific times or depths. Time slices were generated for times 2 – 3 ns, 4 – 5 ns, 6 – 7 ns and 9 – 10 ns (Fig. 7). The slices can be divided in four sections A_1, A_2, A_3 and A_4. Small structures are present on section A_1 to the north, which is separated from section A_3 by a pathway. Section A_2 to the east consists of distinct rectangular anomalies. Diagonal walls are observed on the central section A_3, which was not completely imaged due to lack of measurements (shaded region, Fig. 7). The southern section A_4 consists of rectangular structures to the west and diagonal walls to the east.

In conclusion, this high-resolution geophysical study showed that potential targets can be delineated through the application of complementary methods, namely by combining the results of the ground penetrating radar, seismic refraction, surface waves and electrical tomography techniques.

Acknowledgements

We thank the Department of Mineral Resources Engineering, Technical University of Crete for covering data acquisition cost. We also thank the French School of Archaeology, Athens for providing access to the archaeological site and Prof. S. Mertikas for providing GPS data.

References

HAENI, F. P., GRANTHAM, D. G. AND ELLEFSEN, K., 1987, Microcomputer-based version of Sipt-. A program for the interpretation of seismic-refraction data. Open file report 87-103-A. Harford, Connecticut.

LOKE, M. H. AND BARKER, R.D., 1995, Least squares deconvolution of apparent resistivity pseudosections. *Geophysics, 60*, p. 1682 – 1690.

SCHWAB, F. AND KNOPOFF, L., 1972, Fast surface wave and free mode computations, in Bolt, B. A., Edition, Methods in computational physics, Academic Press, p. 87 – 180.

TELFORD, W. M., GELDART, L. P., SHERIFF, R. E. AND KEYS D. A., 1976, Applied Geophysics, 1st Edition, Cambridge University Press, p. 25 – 28.

VAFIDIS, A., MANAKOU, M., KRITIKAKIS, G. AND VOGANATSIS, D., 2002, The detection of the ancient port in the archaeological site of Itanos (Greece) using shallow seismic methods, *Archaeological Prospection*, submitted for publication.

XIA, J., MILLER, R. D. AND PARK, C. B., 1999, Estimation of near-surface shear-wave velocity by inversion of Rayleigh waves, *Geophysics 64*, No 3, p. 691 – 700.

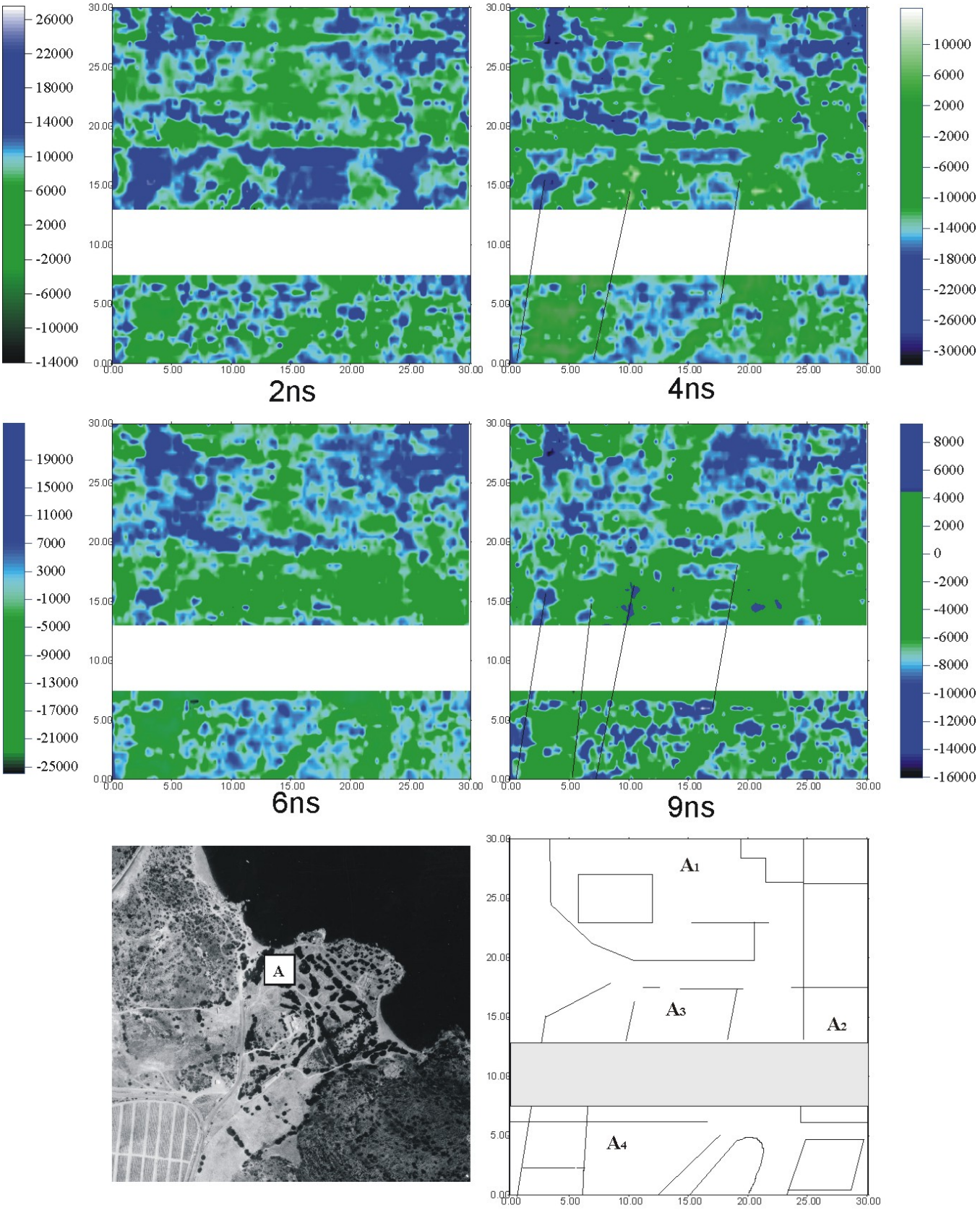

Aerial photo showing Grid A Interpretation

Fig. 7. *Selected time slices, extracted from the 225 MHz radar data, for times 2 – 3 ns, 4 – 5 ns, 6 – 7 ns and 9 – 10 ns. Slices exhibit horizontal variation of the reflected wave amplitudes at specific times or depths. The interpretation of these slices is summarized on the bottom-right image.*